An ultra-spatially resolved method to quali-quantitative monitor particulate matter in urban environment

Chiara Baldacchini[1,2,*], Gregorio Sgrigna[1], Woody Clarke[3], Matthew Tallis[3], Carlo Calfapietra[1,4]

1 Institute of Research on Terrestrial Ecosystems, National Research Council, Via G. Marconi 2, 05010 Porano (TR), Italy

2 Biophysics and Nanoscience Centre, DEB, Università degli Studi della Tuscia, Largo dell'Università, 01100 Viterbo, Italy

3 School of Biological Sciences, University of Portsmouth, King Henry Building, King Henry 1 Street, Portsmouth, PO1 2DY, United Kingdom

4 Department of Landscape Design and Sustainable Ecosystems, Agrarian-technological Institute, RUDN University, 117198, Miklukho-Maklaya Str., 6, Moscow, Russia

[*] Corresponding author: email: chiara.baldacchini@cnr.it; telephone: +39 0763 374933; fax: +39 0763 374980.

Acknowledgments

The publication was financially supported by the Ministry for Education, University and Research of Italy (PRIN 20173RRN2S), by the Ministry of Education and Science of the Russian Federation (Agreement N°02.A03.21.0008) and by the EC Erasmus+ Capacity Building Menvipro. The authors acknowledge project PON infrastructure I-Amica (High Technology Infrastructure for Climate and Environmental Monitoring; PONa3_00363) for the availability of the SEM-EDX facility. Woody Clarke was supported by a Faculty bursary from the University of Portsmouth and a work placement grant funded by EC Erasmus+. Anna Rita Bizzarri and Salvatore Cannistraro (Università degli Studi della Tuscia, Viterbo) are acknowledged for providing the conductimeter. Alessandro Feliziani and Maria Grazia Agrimi (Università degli Studi della Tuscia, Viterbo) are acknowledged for preliminary contribution to conductivity measurements. Martina Ristorini and Silvia Canepari (Università degli Studi di Roma "La Sapienza") are acknowledged for scientific discussions.

Abstract

Monitoring the amount and composition of airborne particulate matter (PM) in the urban environment is a crucial aspect to guarantee citizen health. To focus the action of stakeholders in limiting air pollution, fast and highly spatially resolved methods for monitoring PM are required. Recently, the trees' capability in capturing PM inspired the development of several methods intended to use trees as biomonitors; this results in the potential of having an ultra-spatially resolved network of low-cost PM monitoring stations throughout cities, without the needing of on-site stations. Within this context, we propose a fast and reliable method to qualitatively and quantitatively characterize the PM present in urban air based on the analysis of tree leaves by scanning electron microscopy combined with X-ray spectroscopy (SEM/EDX). We have tested our method in the Real Bosco di Capodimonte urban park (Naples, Italy), by collecting leaves from *Quercus ilex* trees along transects parallel to the main wind directions. The coarse ($PM_{10-2.5}$) and fine ($PM_{2.5}$) amounts obtained per unit leaf area have been validated by weighting the PM washed from leaves belonging to the same sample sets. PM size distribution and elemental composition match appropriately with the known pollution sources in the sample sites (i.e., traffic and marine aerosol). The proposed methodology will then allow to use the urban forest as an ultra-spatially resolved PM monitoring network, also supporting the work of urban green planners and stakeholders.

Keywords

Particulate Matter; Air Quality; Pollution Monitoring; Urban forest; Scanning Electron Microscopy; Energy-resolved X-ray Spectroscopy.

Introduction

Air pollution represents the biggest environmental risk to health (World Health Organization 2016). Air pollution is a complex mixture of gases and particulate matter originating from a variety of sources. Particulate matter (PM) is defined as solid or aqueous compounds in the air, consisting of a multitude of shapes and is classified by mean of the aerodynamic diameter (therefore: PM_{10} is ≤10 µm, $PM_{2.5}$ is ≤2.5 µm). In 2015, exposure to the PM2.5 component of air pollution was estimated to be the highest ranking environmental/occupational risk-factor and the fifth highest ranking overall risk factor of globally mortality, responsible for an estimated 4.2 million deaths globally (Cohen et al. 2017). Cities are severely affected by pollution, especially rapidly growing cities in industrialising countries (Landrigan et al. 2018) and recent estimates suggest 92% of the world population were living in places where the World Health Organization (WHO) air quality guidelines for $PM_{2.5}$ were not met (World Health Organization 2016). Assessed from across a range of global urban environments, it is estimated that 25% of $PM_{2.5}$ is attributed to road traffic, 15% is industrial, 20% is due to domestic fuel burning and 22% is unspecified (Karagulian et al. 2015). Road traffic derived PM are associated with engine emissions, brake and tyre-wear and road surface abrasion, each with their own signatures of particulate size fractions and chemical compositions (Pant and Harrison 2013), and such particles exhibit higher concentrations in the atmosphere near the road (Beevers et al. 2013). Epidemiological studies have identified such anthropogenic particulates to be associated with respiratory conditions such as asthma, chronic bronchitis, and also with strokes, many cancers and dementia (Pope et al. 2002; World Health Organization 2016; Maher at al. 2016; Fuks et al. 2016). By 2050, it is predicted that 68% of the global population will be urban (United Nation 2018) and exposure to anthropogenic urban air pollution, and particularly PM, represents one of the most imminent environmental risks to public health. In this connection, WHO recommends: “Strengthening capacities of cities to monitor their air quality with standardized methods, reliable and good quality instrumentation, and sustainable structures is key.” (World Health Organization 2016).

This study reports an evaluation of analytical approaches to assess the potential for using leaves as filters and samplers of urban atmospheric PM. The use of vegetation as a cost effective strategy to reduce air pollution has a long history (Beckett et al. 1998). The removal of airborne PM through interception by leaves has been widely studied in an attempt to help reduce the negative health impacts associated with urban PM, by urban greening (e.g. Nowak et al. 2006). Decades of such deposition studies have been recently summarised in a meta-analysis by Cai et al. (Cai et al. 2017), reporting urban leaves to accumulate between 3–5 g of PM per m^2 of leaf surface and identifying the fine particulates ($PM_{2.5}$) to be the highest representation of total PM on leaves with respect to particle numbers, but lowest with respect to particle mass. This study also calculated that PM deposition to leaves was in a dynamic equilibrium with the environment after 10 days of no precipitation (Cai et al. 2017), a finding similar to the 6 days identified by Mitchell et al. (Mitchell et al. 2010). Such characteristics suggest leaves to be good passive samplers of local PM.

Any technique using leaves as passive samplers of airborne PM will need to be accurate, precise, repeatable, reproducible and chemically informative. The process must characterise size, numbers and chemical composition of the particulates to be relevant for the monitoring of urban PM related to citizens' health. Vacuum filtration (VF) has been used most extensively (e.g. Dzierżanowski et al. 2011; Sæbø et al. 2012; Sgrigna et al. 2015; Song et al. 2015; Mo et al. 2015; Popek et al. 2017). Using VF, different filters with the respective pore sizes approximate the PM mass into size fractions, e.g. PM_{10} or $PM_{2.5}$. However, because the PM is agglomerated upon the filter surface, the particle numbers, size distribution and chemical composition are rarely quantified (Sgrigna et al. 2016). Additionally, as this is an aqueous filtration, soluble fractions, can be unaccounted for on filter deposition (Freer-smith et al. 2005). Atomic absorption spectroscopy (AAS), gas chromatography - mass spectrometry (GC-MS) and inductively coupled plasma – mass spectrometry (ICP-MS) can be used for chemical analysis but are limited in details of particle size and numbers (De Nicola et al. 2008; Sawidis et al. 2011; Simon et al. 2014). Also biomagnetic monitoring of atmospheric pollution accumulated on biological surfaces is a growing application in the field of environmental magnetism, providing a record of location-specific, time-integrated air quality information, mainly through saturation isothermal remanent magnetization (SIRM) (Hofman et al. 2017), but no information on particle morphology can be obtained. Using leaves as *in situ*, low-cost, highly spatially resolved passive samplers for monitoring urban PM, scanning electron microscopy combined with energy dispersed X-ray spectroscopy (SEM/EDX) has been reported to be the most appropriate analytical technique to study PM size, number and chemical composition directly on the leaves of urban trees (Wang et al. 2015; Yan et al. 2016; Baldacchini et al. 2017) or shrubs (Weerrakkody et al. 2018; Shao et al. 2019). However, the spatial scale of a SEM/EDX analysis (typically hundreds of microns square of leaf area per sample) is very limited compared to the more commonly used VF (typically many leaves per sample) and no quantitative estimation of the PM amount in terms of mass has been reported by this technique up to date.

This study investigates the deposition of coarse ($PM_{10\text{-}2.5}$) and fine ($PM_{2.5}$) particles on the leaves of evergreen Holm Oak (*Quercus ilex*) trees in an urban park in Naples (Italy), at varying proximity to potential PM pollution sources and along the two main wind directions (one of which is from the sea). A method to provide mass estimation of leaf deposited PM using SEM/EDX is proposed and validated by the comparison with data obtained by VF from the same samples. Further, electron conductivity (EC) was used to estimate the quantity of total dissolved solid (TDS) in the filtrate, typically unrepresented in the VF technique.

Materials and Methods

Leaf sampling

The sampling campaign took place in Real Bosco di Capodimonte (February 1st, 2017), an urban forest within Naples, Italy (40.8725° N, 14.2533° E). Seven different locations within the forest (Figure 1a) were selected along the two main wind directions (Figure 1b and 1c), within an area less than 5 ha wide. Locations were chosen by the following criteria: location 1 within the wood, locations 2 and 4 adjacent to a busy street, locations 3 and 5 on the border between wood and meadow, 6 and 7 on the border between wood and brownfield. Single *Quercus ilex* (Holm Oak) trees were selected at each location. The aspect of the canopy that was sampled was selected according to the prevailing wind directions: North-West winds from urban and industrial areas dominating influence on the canopy sampling at locations 2, 3 and 6; South-West wind direction from the coastline of Naples dominating influence on canopy sampling at locations 1, 4, 5, and 7. Two replicate branches were taken from each tree, at a height of 8 m. New leaves, approximated to be 8 months old, were sampled to ensure that the PM accumulation is from recent deposition, comprising of 58 (± 17) leaves per branch, with an average leaf area of 452 cm^2 (SD ±82 cm^2). Leaf samples were stored in sealed bags at -20°C for three months prior to analysis.

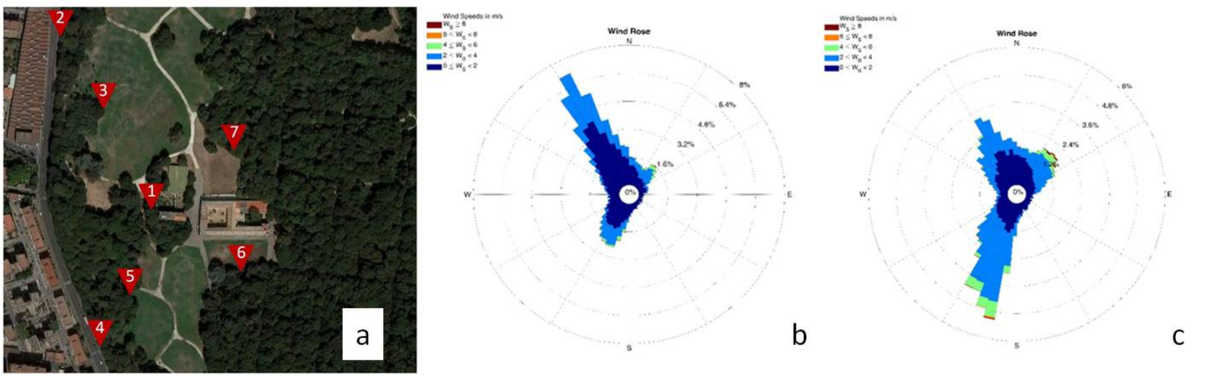

Fig. 1 a) Sampling locations across the urban forest of Real Bosco di Capodimonte (Naples, Italy). Rose wind diagrams describing wind direction and speed at night (b) and day (c).

Scanning electron microscopy and energy-dispersive X-ray spectroscopy

A Phenom ProX (Phenom-World, The Netherlands) scanning electron microscope was used, equipped with X-ray analyzer and charge-reduction sample holder suited for biological samples. Two leaves were selected from each replicate branch, giving a total of 28 leaves used for SEM/EDX analysis. An approximately 1 x 1.5 cm^2 portion of each leaf was selected per sample and fixed to the head of carbon-based stub (PELCO Tabs, Ted Pella, Inc.), with the adaxial leaf surface pointing upwards, after having fluxed them with compressed air.

For particulate size analysis and number count, SEM images were performed in backscattered electron configuration, with an incident electron energy of 5 keV, in order to limit the surface charging. Ten random images, with an approximate area of 150x150 μm^2 (1024x1024 pixels), were taken for each sample (280 images in total). Each selected image was analysed using Gwyddion open source software (Nečas et al. 2012). By applying a colour threshold based grain analysis (Yan et al. 2016; Baldacchini et al. 2017), the number of particles in the image, together with the aerodynamic diameter (diameter of the equivalent sphere, d_{eq}) of each particle, were obtained. Particles with a d_{eq} comparable with the size of a single pixel (0.146 μm) were excluded, resulting in a lower cut-off at about 0.3 μm in the diameter of the analysed particles. Particles with a d_{eq} larger than 10 μm (which accounted for less than 0.1% of the total detected particles) were also excluded, resulting in a final data set composed by $PM_{10\text{-}0.3}$ particles.

For the elemental analysis of the leaf deposited particles, five images with a lateral size of 50 μm (1024x1024 pixels) per sample were further acquired, in backscattered electrons configuration and at an electron voltage of 15 kV. Ten particles were randomly chosen per each image, resulting in a total of 50 particles for each leaf sample and, including each replicate, a total of 200 particles per sampling location. Per each particle, d_{eq} was obtained by averaging their two main Feret diameters (Merkus 2009), as measured by ImageJ software (Schneider et al. 2012), and, through dedicated Phenom Pro Suite software, the corresponding EDX spectrum was obtained by positioning the laser beam in the particle center (Baldacchini et al. 2017). The main elements identified in the PM are C, N, O, Na, Mg, Al, Si, Cl, K, Ca, Ti, and Fe. Trace elements (F, P, S, Cr, Mn, Co, Ni, Cu, Zn, Sr, Mo, Sn, Sb, Ba, and Bi) have been also observed. An estimation of the PM elemental composition was obtained by calculating the weighted volume percentage ($W_{\%}$) occupied by each element x over the number of selected particles, outlined in equation Equation 1 (Sgrigna et al. 2016; Baldacchini et al. 2017). For each location n, $W_{\%n}$ was obtained as the product of the relative percentage of each element x in each particle i (C_{xi}, as obtained by the EDX software) and the corresponding particle volume $V_i = 4/3\ \pi\ (d_{eqi}/2)^3$. Then, for each element, the relative volumes occupied in all the analysed particles were summed together, and the sum was normalized by using the total volume of the EDX analysed particles.

$$W_{\%xn} = \frac{\sum_i C_{xi} V_i}{\sum_i V_i} \qquad \text{(Equation 1)}$$

Leaf deposited PM mass estimation was then obtained by multiplying the $W_{\%xn}$ of each element x, at the location n, by the total particle volume at the corresponding location (V_n, as obtained by the SEM images of the collected leaves) and by the corresponding elemental atomic mass per volume (am_x, also known as solid state density; values have been taken from https://www.webelements.com/periodicity/density/). The obtained quantity was then normalized by the total imaged area (A_n) multiplied by a factor of 1.5, to take into account that images have been acquired only on the adaxial leaf side, while PM accumulation occurs on both leaf sides, with the abaxial one being able to accumulate almost half of the PM quantity with respect to the other (Baldacchini et al. 2017). The resulting quantity is the PM load per unit leaf area (µg cm^{-2}, M_n):

$$M_n = \sum_x \frac{W_{\%xn} \cdot V_n \cdot am_x}{1.5 A_n} \qquad \text{(Equation 2)}$$

Vacuum filtration

The VF analysis was conducted as previously described (Sgrigna et al. 2015). Ten leaves from each replicate branch and sampling location were selected for the VF procedure. Leaf samples were thoroughly shaken in a flask, with 250 ml of de-ionised water, for 5 minutes. Washed leaves were then scanned and leaf surface area measured using ImageJ. The wash water was pre-filtered through a 100 µm pores sieve and then pulled by a vacuum pump though cellulose filters with a pore size of 10-15 µm (Anoia S.A., Barcelona, code 1250) measuring the size fraction between 10 and 100 µm, then though filters with a pore size of 2-4 µm (Anoia S.A., Barcelona, code 1244) measuring the size fraction 2-10 µm, and finally though nitrocellulose membranes (Advanced Microdevices Pvt. Ltd, type: CN-S) for 0.2 µm measuring the size fraction 0.2-2 µm.

All filters were dried in a moisture controlled oven (Griffin Company) for 40 minutes at 70°C and were placed into the balance room for 30 minutes before obtaining the mass, to equilibrate to humidity levels. The dried mass of filters was obtained (Sartorius moisture laboratory) at precision of x10^{-5} g before (T_1) and after (T_2) filtration. The mass of leaf deposited PM per unit leaf area was then estimated for each respective size fraction as the difference between T_2 and T_1 masses, further divided by the total two-sided leaf area washed (µg cm^{-2}).

Total dissolved solid determination

The EC of wash solution after the 0.2 µm membrane filtration was measured (Crison Basic 30 conductimeter, equipped with standard 5070 platinum cell). Normalized values of the EC, taking account of the measuring temperature, are provided by the instrument and used to estimate the TDS (mg ml^{-1}) by multiplying the EC by the fresh water conversion factor (0.65; Rusydi 2018). For TDS values to be compared with the mass values obtained by the two other techniques, these were multiplied by the total volume of the wash solution (0.25 litres) and divided by the total two-sided washed leaf area (and expressed as µg cm^{-2}).

Data analysis

Correlation and principal component (PC) analyses have been performed on the $W_{\%}$ data of the most abundant elements, i.e. those having $W_{\%}$ higher than 0,1% at each location (namely, Na, Mg, Al, Si, Cl, K, Ca, Ti, Fe), for three PM size fractions (PM10-2.5, PM2.5-1.0, PM1.0-0.3). Statistica v 8 (StatSoft Italia srl, Padua, Italy) software has been used. C, N, and O were excluded from the analysis since they can be related to biogenic factors and EDX is known to fail in the correct determination of these light elements (Wilkinson et al. 2013, Baldacchini et al. 2017). For mass load correlation analysis among techniques, Origin v.8.1 (OriginPro) software has been used.

Results and discussion

The mean particle densities per unit leaf area of $PM_{10-0.3}$, as estimated by the SEM imaging and grain analysis over the 4 replicates per the 7 locations, are shown in Fig.2a. The lowest particle densities (about 1 x 10^5 particles/mm^2) are observed at the inner park locations (1 and 5), and this value was doubled for the particle density observed at the locations along the high traffic density street (2 and 4). Location 6 and 7, which are located at the border between a small woodland and a brownfield, have intermediate particle density values, comparable between them. Inner park location 3 shows a particle density comparable with the roadside locations. The observed particle densities are similar to those previously reported for PM deposition on *Tilia cordata* leaves, along a 5-months sampling campaign performed in Parma (Mantovani et al., 2018), while they are large if compared with those obtained by using *Platanus acerifolia* as sampling species (Baldacchini et al. 2017). In this latter case, values as high as 10^5 particles/mm^2 were observed only in critically polluted and dry cities (i.e., Yerevan), while in Naples the leaf particle density was about 2-3 x 10^4 particles/mm^2. However, such a variability in the leaf deposited particle density is not surprising: it may depend on several factors, such as the sampling sites and the sampling period, as well as on the sampling species. Indeed, different species can be characterized by different capturing capability, likely due to leaf macro and micro morphological differences (Kardel et al. 2011, Sæbø et al. 2012, Wang et al. 2013, Mo et al. 2015, Chen et al. 2017).

The distribution over the three main particle size fractions ($PM_{10-2.5}$, $PM_{2.5-1.0}$ and $PM_{1.0-0.3}$) is reported in Fig.2b. All the locations have similar particle size distribution, with about 90% of the particles having an aerodynamic diameter below 1.0 µm ($PM_{1.0-0.3}$), from 5% to 10% belonging to the $PM_{2.5-1.0}$ fraction and less than 2% of coarse particles ($PM_{10-2.5}$); these values being similar to those previously reported for *P. acerifolia* (Baldacchini et al. 2017) and being consistent with the typical atmospheric PM size fraction distribution observed, for instance, by optical particle counters (Tittarelli et al. 2008). Location 3 shows a relatively high percentage of $PM_{2.5-1.0}$ (18%) that, together with the unexpected high particle density observed, would suggest that the sampled leaves could be older than those collected at other locations; this possibly implying a higher number of particles on the leave surfaces and clustering of fine PM in larger particles.

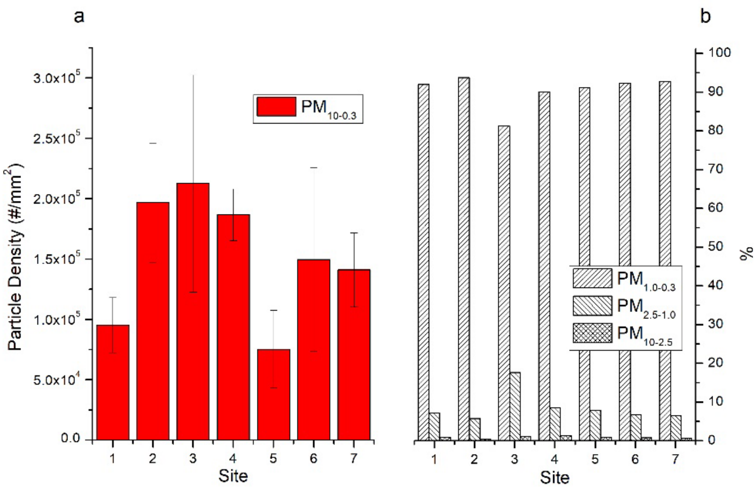

Fig. 2 A description of total particle density (a) and particle size distribution (b) across locations, as estimated from grain analysis of the SEM images of adaxial *Q. ilex* leaf surfaces.

The elemental composition of PM belonging to the three size fractions is shown in Fig. 3. At every location, with decreasing the PM size, the $W_{\%}$ of the main crustal elements (Al and Si) decreases, with a corresponding increasing of the Fe $W_{\%}$. At every size fraction, the Fe $W_{\%}$ content is from three to four times larger in locations 2 and 4, the roadside ones, with respect to the other locations. It increases from 4.60% and 9.15% ($PM_{10-2.5}$) to 9.08% and 11.52% ($PM_{2.5-1.0}$) and to 10.94% and 14.41% ($PM_{1.0-0.3}$), for location 2 and 4, respectively. A $W_{\%}$ of over 5% of Fe has been described as predictive of roadside pollution footprint (Baldacchini et al. 2017). Indeed, airborne particles in the proximity of high traffic roads are characterized by high Fe content, likely due to brake consumption, as previously verified, for instance by ICP-MS on impactor collected PM (Harrison et al. 2012).

Correlation analysis has been performed among those elements having $W_{\%}$ higher than 0,1% at each location (namely, Na, Mg, Al, Si, Cl, K, Ca, Ti, Fe), for the three PM size fractions. Significant ($p < 0.05$) positive correlations have been obtained: in $PM_{10-2.5}$, for Na and Cl ($r = 0.97$) and for Ca and Ti ($r = 0.85$); in $PM_{2.5-1.0}$, for Na and Cl ($r = 0.82$), for Mg and Ca ($r = 076$), Ca and Ti ($r = 0.89$), Ca and Fe ($r = 0.94$), and for Ti and Fe ($r = 0.82$); in $PM_{1.0-0.3}$, for Na and Cl ($r = 0.78$), for Al and Si ($r = 0.79$), and for K and Cl ($r = 0.86$). It is worth noting that significant correlation between Na and Cl $W_{\%}$ is obtained at every size fraction, likely due to marine aerosol deposition on leaves (Baldacchini et al. 2017), with some of the selected locations being exposed to marine breeze from South-West during the day. High and correlated concentrations of Na^+ and Cl^- have been previously reported as due to marine breeze also in airborne particles collected by gravimetric techniques and analyzed by chromatography (Yin et al. 2005).

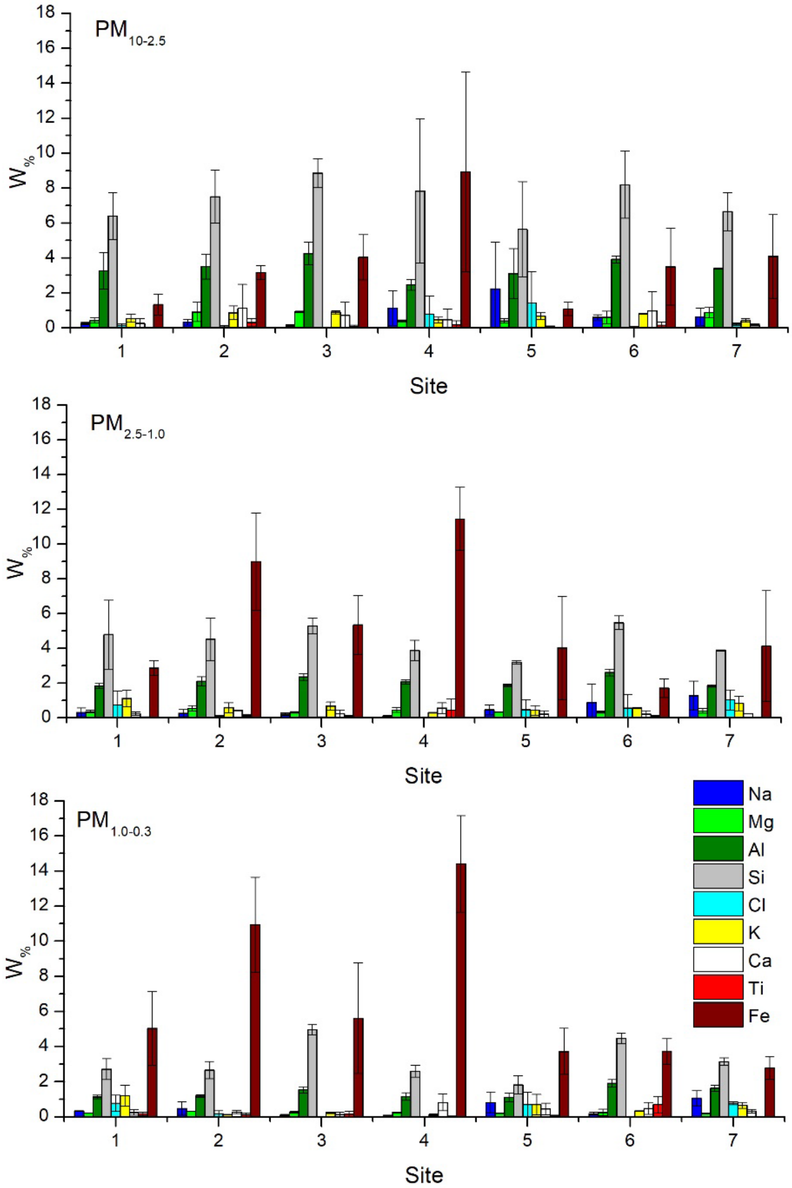

Fig. 3 The elemental composition, estimated by elemental $W_{\%}$ from the SEM/EDX analysis, for the three PM size fractions (10-2.5 μm, 2.5-1.0 μm, 1.0-0.3 μm) from all sampling locations.

Principal component analysis (PCA) based on correlation, applied to the $W_{\%}$ data of the selected elements, for the three PM size fractions, highlights the most location discriminant elements. The factor coordinates (Fig. 4a, c and e) and the factor scores (Fig. 4b, d and f) of the two first PCs are plotted in Fig. 4, for the three PM size fractions. The eigenvalues of the two principal components (PCs), measuring proportion of variance, are at 52.55% and 22.58% for $PM_{10\text{-}2.5}$, 51.54% and 23.02% for $PM_{2.5\text{-}1.0}$, 42.99% and 30.32% for $PM_{1.0\text{-}0.3}$, for PC1 and PC2 respectively. At the three size fractions, according to the correlation analysis, PC1 mainly describes the clustering of sites dominated by the correlated presence of Na and Cl (1, 5 and 7). PC2, instead, discriminates, at the three sites fractions, sites dominated by "crustal components" such as Al and Si (sites 3 and 6) from those presenting high Fe concentration (2 and 4). Only in $PM_{10\text{-}2.5}$ location 2 is grouped with 3 and 6 instead of 4, likely due to the fact that coarse PM results from the aggregation of fine PM with different source apportionment.

The behaviour of the remaining elements (Mg, K, Ca, Ti) is not straightforward, probably because they are characterized by lower $W_{\%}$ and may have different origins, either natural and anthropogenic (Sgrigna et al. 2016). As a consequence, they correlate with different elements in the different size fractions, but without discriminant power: PCA performed by eliminating these elements one by one displayed no differences in the location clustering.

The clustering of sites 1, 5 and 7 at each PM size fraction, according to the correlated presence of Na and Cl, reveals that leaves have been sampled from the canopy facing the prevailing sea breeze from South-West at these locations. On the other side, locations 3 and 6 are correctly characterized by high concentrations of Al and Si, which could be associated with soil or earth compounds, since leaves have been sampled from the canopy side exposed to wind from North-West and protected with respect to the marine breeze. Finally, the cluster explained by high Fe concentration (typical of roadside combustion particulates, as previously said) is associated with roadside and road-facing canopy leaves from locations 2 and 4.

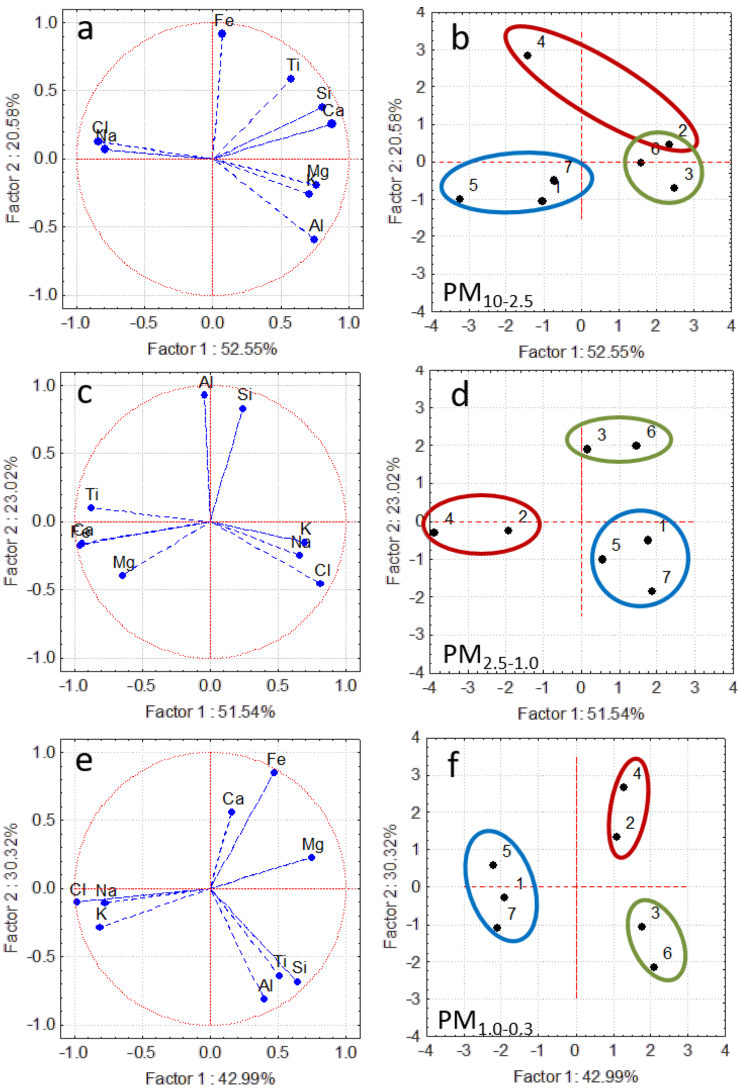

Fig. 4 Biplots of the factor coordinates of variables (a, c, e) and of factor scores (b, d, f) of the two first PCs obtained by correlation PCA of the elemental $W_{\%}$ for the $PM_{10\text{-}2.5}$ (a, b), $PM_{2.5\text{-}1.0}$ (c, d) and $PM_{1.0\text{-}0.3}$ (e, f) size fractions.

The PM mass per unit leaf area (i.e., the particle load) as estimated by combining SEM and EDX data is shown in Table 1, for each location. The corresponding particle loads as obtained by VF by using leaves from the same sampling collections are reported in Table 2. The results obtained with the two techniques can be directly compared for the coarse particles' fraction (which is $PM_{10\text{-}2.5}$ for SEM/EDX and $PM_{10\text{-}2.0}$ for VF), while the fine particles' fraction obtained by VF ($PM_{2.0\text{-}0.2}$) contains both the two finest fractions of the SEM/EDX analysis ($PM_{2.5\text{-}1.0}$ and $PM_{1.0\text{-}0.3}$). The mean particle loads obtained for coarse and fine PM with the two techniques are compared in Fig.5a.

Table 1 The estimated mass of PM on leaves, per unit leaf area, as obtained from SEM/EDX, as average values over the two replica. Standard deviation (SD) is given for each estimation at the different seven sites. The value averaged over the seven sites, at each PM size fraction, is given with standard error (SE).

	PM mass per unit leaf area estimated by SEM/EDX (µg/cm^2) (± SD)							
	1	2	3	4	5	6	7	Mean ± SE
$PM_{10\text{-}2.5}$	3.9 ± 01.3	4.1 ± 1.9	9.3 ± 5.0	16.7 ± 7.3	2.9 ± 2.1	5.9 ± 3.6	6.4 ± 5.6	7.0 ± 1.8
$PM_{2.5\text{-}1.0}$	1.8 ± 0.5	3.3 ± 0.7	4.6 0.4	5.6 ± 0.7	1.7 ± 0.2	2.6 ± 1.3	2.6 ± 0.6	3.2 ± 0.6
$PM_{1.0\text{-}0.3}$	0.9 ± 0.3	2.1 ± 0.1	2.1 ± 1.2	2.3 ± 0.3	0.7 ± 0.2	1.3 ± 0.7	1.2 ± 0.3	1.5 ± 0.2

Table 2 The estimated mass of PM on leaves, per unit leaf area, as obtained from VF, as average values over the two replica. Standard deviation (SD) is given for each estimation at the different seven sites. The value averaged over the seven sites, at each PM size fraction, is given with standard error (SE).

	PM mass per unit leaf area estimated by VF (µg/cm^2) (± SD)							
	1	2	3	4	5	6	7	Mean ± SE
$PM_{10\text{-}2.0}$	0.44 ± 0.11	1.77 ± 0.51	1.28 ± 0.19	1.18 ± 0.16	0.37 ± 0.03	0.81 ± 0.01	0.06 ± 0.6	0.8 ± 0.2
$PM_{2.0\text{-}0.2}$	3.66 ± 0.12	2.95 ± 1.02	5.21 ± 0.05	3.73 ± 0.90	6.41 ± 0.23	5.55 ± 0.88	4.64 ± 1.67	4.6 ± 1.2

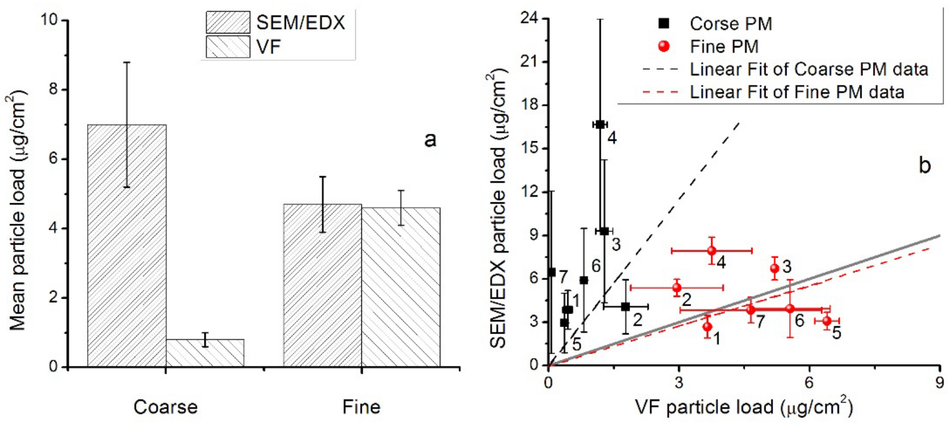

Fig. 5 (a) Mean particle loads of coarse and fine PM over the sampling set, as obtained by SEM/EDX and VF. Error bars represent the standard error. (b) Coarse (black squares) and fine (red circles) PM loads estimated by SEM/EDX plotted as a function of the corresponding value estimated by VF, per each sampling location. The dashed lines represent the corresponding best linear fits, as obtained separately for the coarse fraction (black line; slope = 3.8 ± 1.2, R^2 = 0.55) and the fine fraction (red line; slope = 0.91 ± 0.22, R^2 = 0.70). The grey thick line (slope = 1) guides the eye to identify the ideal 1:1 correlation between the datasets.

Averaged across all sites, the two techniques strongly agree in the determination of fine PM load, which is 4.7 ± 0.8 µg/cm^2 by SEM/EDX and 4.6 ± 1.2 µg/cm^2 by VF, and these values are further consistent with a previous study performed by using *Q. ilex* to monitor PM in the industrial city of Terni (Italy) by VF (Sgrigna et al. 2015). However, they completely disagree in the coarse PM quantification: the coarse PM load is greater than that of fine PM when determined by SEM/EDX (7.0 ± 1.8 µg/cm^2), as expected (Cai et al. 2017), while an inverted *ratio* is observed when VF is used (VF determined coarse PM load is 0.8 ± 0.2 µg/cm^2). The total PM_{10} load obtained (summed mass of all particulates ≤ 10 µm) is 11.7 ± 2.5 µg cm^{-2} by SEM/EDX and 5.4 ± 0.9 µg cm^{-2} by VF. The previous VF study performed on *Q. ilex* obtained a coarse PM load of about three times the fine PM load, resulting in a mean total PM_{10} load of about 20.6 µg cm^{-2} (Sgrigna et al. 2015). An higher coarse PM load was generally observed also by two further studies studying fine and coarse PM loads by VF on a wide range of tree species in China (Mo et al. 2015) and in Norway and Poland (Sæbø et al. 2012). The mean PM_{10} load in these cases was about 12 µg cm^{-2} (Mo et al. 2015) and ranged between 4 and 17 µg cm^{-2}, depending on the sites (Sæbø et al. 2012), respectively. All these mean PM_{10} load values are highly consistent with our SEM/EDX estimates. However, some exceptions showing coarse PM load lower than fine PM load have been also reported by the two latter studies, mainly depending on the tree species.

The PM load location-dependent analysis is shown in Fig.5b, where the values obtained by SEM/EDX for both the coarse and the fine PM load, at each location, are plotted as a function of the corresponding VF results. Again, a close parity between the two techniques is obtained for the fine PM estimates of mass (red circles), as represented by the trend of scatter around the 1:1 line (grey line in Fig.5b); the best linear fit of the fine PM results (red dashed line, $R^2 = 0.70$) having a slope of 0.91 ± 0.22. On the contrary, for the coarse PM, the SEM/EDX value is always higher than the corresponding VF value (black squares). With the intercept forced through zero, the gradient of the positive linear relationship (black dashed line, $R^2 = 0.55$) is 3.8 ± 1.2, indicating that the mass estimation by SEM/EDX is almost four times higher than that of VF for the coarse PM fraction. A possible explanation for this different estimation could reside in the soluble part of PM, which is lost, or fragmented, in VF. Indeed, the sites with prevailing PM contribution from the marine aerosol (1, 5, and 7), which is predominantly salt (NaCl), are those showing the lowest coarse PM load by VF.

Salt dissociation should result in an enhancement of the electrical conductivity (EC) of the wash solution, proportional to the quantity of dissolved ions, *i.e.* of the washed salt. The total dissolved solid (TDS) estimates obtained by the EC measurements of the wash solutions, combined with the VF determined PM_{10} loads (VF+TDS), are compared with the corresponding SEM/EDX estimates in Fig. 6. The total (VF+TDS) PM_{10} load is quite homogeneous over the locations, with a mean value of 13.0 ± 1.5 μg cm^{-2}, while the SEM/EDX estimate is more scattered, having a mean value of 11.7 ± 2.5 μg cm^{-2}. However, the two mean estimates are now in agreement, as well as five of the sites' estimates (2, 3, 4, 6 and 7). Only locations 1 and 5 exhibit a disparity between the techniques, likely due to the rough TDS estimation performed, which largely affects those sites with major salt contribution in the PM load. Moreover, locations 1 and 5 have the lowest Fe $W_{\%}$: a total estimate of 1.62 ± 0.30 and 1.99 ± 0.97, respectively, as compared with an average of 4.15 and maximum of 9.15 in location 4 (road-side). Since SEM/EDX sensitivity improves with the atomic weight, a general underestimation of PM load by SEM/EDX at low Fe $W_{\%}$ locations cannot be excluded.

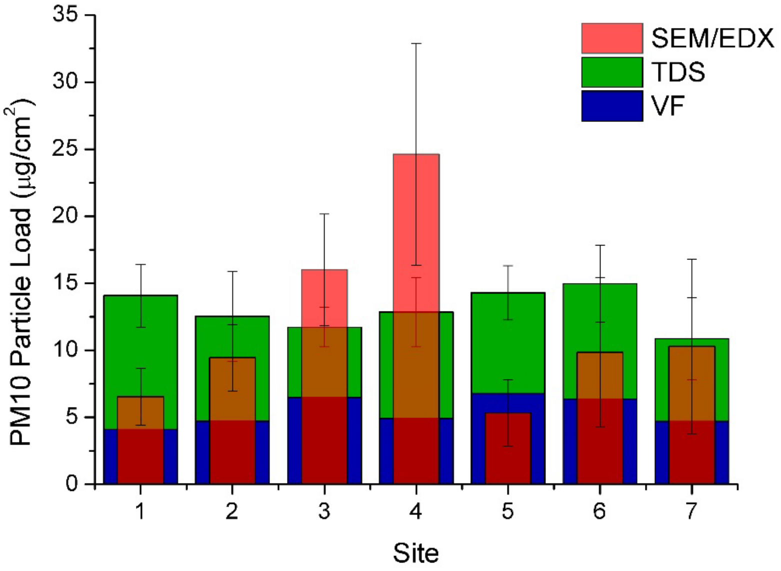

Fig. 6 A comparison of estimated PM_{10} load by SEM/EDX ($PM_{10-0.3}$) and by combined VF ($PM_{10-0.2}$) and TDS.

Conclusions

This study reports a detailed evaluation of a new analytical approach to assess the potential of tree leaves as passive samplers for *in situ*, low-cost, highly spatially resolved urban PM monitoring. In particular, tree leaves and SEM/EDX have been identified as a highly spatially resolved system with the capability to inform on particulate size, frequency distribution of sizes classes and elemental composition of atmospheric PM. By accurately sampling the tree canopy with respect to the main wind directions, we have obtained very different results, highly indicative of the source apportionment, within a 5 ha area of the same urban park. North-West wind flux from the outskirts of the city of Naples mainly brings elements of natural origin (crustal elements) such as Al and Si. The South-West wind flux is from the sea, notably containing the Na and Cl elements. High Fe deposition ($W_{\%} > 10\%$) characterizes the areas typical of heavy traffic.

Moreover, an original method to obtain PM mass deposition estimates from SEM/EDX measurements of leaf deposited PM has been presented and validated. For fine PM ($PM_{2.5}$), the provided estimates are generally comparable to those obtained with VF, which determines the PM load from whole leaf washing and therefore offers the potential of a large sample size. Discrepancies have been obtained in the coarse PM ($PM_{10-2.5}$) mass determination. This could be due to the loss of the soluble part of PM during VF, as demonstrated by measuring the EC of the wash solution. However, EC can take into account only the ionic part of the solved PM and further studies are in progress to include also non-ionic compounds in this analysis. Moreover, to disclose the efficiency of the presented method in quantifying PM as a function of its elemental composition and/or size fraction, the elemental and ion composition of both leaf deposited PM and wash solution will be further characterized by Inductively Coupled Plasma Mass Spectrometry (ICP-MS) and Inductively Coupled Plasma Optical Emission Spectroscopy (ICP-OES), and by Ion Chromatography (IC), respectively.

The use of SEM/EDX to study leaf deposited PM emerges then as a suitable tool to be used to guide future estimation of PM deposition upon vegetation and support best practise in identifying airborne PM pollution sources within the urban environment. Furthermore, the high spatial resolution provided by this technique offers an approach to allow closer alignment between medical studies of the airborne disease pathway and the reduction by vegetative interception of PM, so informing targeted planting for air quality management.

References

Beckett KP, Freer-Smith PH, Taylor G (1998) Urban woodlands: their role in reducing the effects of particulate pollution. Environ. Pollut. 99:347−360.

Baldacchini C, Castanheiro A, Maghakyan N, et al. (2017) How Does the Amount and Composition of PM Deposited on *Platanus acerifolia* Leaves Change across Different Cities in Europe? Environ. Sci. Technol. 51(3):11471156.

Beevers SD, Kitwiroon N, Williams ML, Kelly FJ, Anderson HR, Carslaw DC (2013) Air pollution dispersion models for human exposure predictions in London. J. Expo. Sci. Environ. Epidemiol. 23(6):647-653.

Cai M, Xin Z, Yu X (2017) Spatio-temporal variations in PM leaf deposition: A meta-analysis. Env. Pol. 231:207-218.

Chen L, Liu C, Zhang L, Zou R, Zhang Z (2017) Variation in Tree Species Ability to Capture and Retain Airborne Fine Particulate Matter (PM2.5). Sci. Rep. 7:3206.

Cohen AJ, Brauer M, Burnett R, Anderson HR, Frostad J, Estep K, Balakrishnan K, Brunekreef B, Dandona L, Dandona R, Feigin V (2017) Estimates and 25-year trends of the global burden of disease attributable to ambient air pollution: an analysis of data from the Global Burden of Diseases Study 2015. The Lancet 389(10082):1907-1918.

De Nicola F, Maisto G, Prati MV, Alfani A (2008) Leaf accumulation of trace elements and polycyclic aromatic hydrocarbons (PAHs) in *Quercus ilex L.* Environ. Pollut. 153(2):376−383.

Dzierżanowski K, Popek R, Gawrońska H, Sæbø A, Gawroński SW (2011) Deposition of particulate matter of different size fractions on leaf surfaces and in waxes of urban forest species. Int. J. Phytoremediation 13:1037-1046.

Freer-Smith PH, Beckett KP, Taylor G (2005) Deposition velocities to *Sorbus aria, Acer campestre, Populus deltoides× trichocarpa 'Beaupré', Pinus nigra and× Cupressocyparis leylandii* for coarse, fine and ultra-fine particles in the urban environment. Environ. Pollut. 133(1):157-167.

Fuks K, Weinmayr G, Basagaña X et al. (2016) Long-term exposure to ambient air pollution and traffic noise and incident hypertension in seven cohorts of the European study of cohorts for air pollution effects (ESCAPE). European Heart Journal 38(2):71-72.

Harrison RH, Jones AM, Gietl J, Yin J, Green DC (2012) Estimation of the Contributions of Brake Dust, Tire Wear, and Resuspension to Nonexhaust Traffic Particles Derived from Atmospheric Measurements. Environ. Sci. Technol. 46:6523−6529.

Hofman J, Maher BA, Muxworthy AR, Wuyts K, Castanheiro A, Samson R (2017) Biomagnetic monitoring of atmospheric pollution: a review of magnetic signatures from biological sensors. Environ. Sci. Technol. 51(12):6648–6664.

Karagulian, F, Belis CA, Dora CFC, Prüss-Ustün AM, Bonjour S, Adair-Rohani H, Amann M (2015) Contributions to cities' ambient particulate matter (PM): A systematic review of local source contributions at global level. Atm. Environ. 120:475-483.

Kardel F, Wuyts K, Maher B, Hansard R, Samson R (2011) Leaf saturation isothermal remanent magnetization (SIRM) as a proxy for particulate matter monitoring: Inter-species differences and in-season variation. Atm. Environ. 45:5164-5171.

Landrigan PJ, Fuller R, Acosta NJ, Adeyi O, Arnold R, Baldé AB, Bertollini R, Bose-O'Reilly S, Boufford JI, Breysse PN, Chiles T (2018) The Lancet Commission on pollution and health. The Lancet 391(10119):462-512.

Maher BA, Ahmed IA, Karloukovski V et al. (2016). Magnetite pollution nanoparticles in the human brain. Proc. Natl. Acad. Sci. USA 113:10797- 10801.

Mantovani L, Tribaudino M, Solzi M, Barraco V, De Munari E, Pironi C (2018) Magnetic and SEM-EDS analyses of Tilia cordata leaves and PM10 filters as a complementary source of information on polluted air: Results from the city of Parma (Northern Italy). Environ. Pollut. 239: 777-787.

Merkus HG (2009) Particle Size Measurements: Fundamentals, Practice, Quality. Springer Science + Business Media B.V.

Mitchell R, Maher BA, Kinnersley R (2010) Rates of particulate pollution deposition onto leaf surfaces: temporal and inter-species magnetic analyses. Environ. Pollut. 158:1472-1478.

Mo L, Ma Z, Xu Y et al. (2015) Assessing the Capacity of Plant Species to Accumulate Particulate Matter in Beijing, China. PLOS ONE 10(10):e0140664.

Nečas D, Klapetek P (2012) Gwyddion: an open-source software for SPM data analysis. Cent. Eur. J. Phys. 10(1):181－188.

Nowak D, Crane D, Stevens J (2006) Air pollution removal by urban trees and shrubs in the United States. Urban Forestry & Urban Greening 4:115–23.

Pant P, Harrison RM (2013) Estimation of the contribution of road traffic emissions to particulate matter concentrations from field measurements: a review. Atm. Environ. 77:78-97.

Pope CA, Burnett RT, Thun MJ, Calle EE, Krewski D, Ito K, Thurston GD (2002) Lung cancer, cardiopulmonary mortality, and long-term exposure to fine particulate air pollution. J. Am. Med. Assoc. 287:1132–1141.

Popek R, Łukowski A, Bates C, Oleksyn J (2017) Accumulation of particulate matter, heavy metals, and polycyclic aromatic hydrocarbons on the leaves of *Tilia cordata Mill.* in five Polish cities with different levels of air pollution. Int. J. Phytoremediation, 19(12):1134-1141.

Rusydi AF (2018) Correlation between conductivity and total dissolved solid in various type of water: A review. IOP Conf. Ser.: Earth Environ. Sci.118:012019

Sæbø A, Popek R, Nawrot B, Hanslin HM, Gawronska H, Gawronski SW (2012) Plant species differences in particulate matter accumulation on leaf surfaces. Sci. Total Environ. 427:347-354.

Sawidis T, Breuste J, Mitrovic M, Pavlovic P, Tsigaridas K (2011) Trees as bioindicator of heavy metal pollution in three European cities. Environ. Pollut. 159(12):3560−3570.

Schneider CA, Rasband WS, Eliceiri KW (2012) NIH Image to ImageJ: 25 years of image analysis. Nature Methods 9:671-675.

Sgrigna G, Sæbø A, Gawronski S, Popek R, Calfapietra C (2015) Particulate Matter deposition on *Quercus ilex* leaves in an industrial city of central Italy. Environ. Pollut. 197:187-194.

Sgrigna G, Baldacchini C, Esposito R, Calandrelli R, Tiwary A, Calfapietra C (2016) Characterization of leaf-level particulate matter for an industrial city using electron microscopy and X-ray microanalysis. Sci. Total Environ. 548-549:91-99.

Shao F, Wang L, Sunc F, Li G, Yu L, Wang Y, Zeng X, Yan H, Dong L, Bao Z (2019) Study on different particulate matter retention capacities of the leaf surfaces of eight common garden plants in Hangzhou, China. Sci. Total Environ. 652:939–951.

Simon E, Baranyai E, Braun M, Cserháti C, Fábián I, Tóthmérész B (2014) Elemental concentrations in deposited dust on leaves along an urbanization gradient. Sci. Total Environ. 490:514−520.

Song Y, Maher B, Li F, Wang X, Sun X, Zhang H (2015) Particulate matter deposited on leaf of five evergreen species in Beijing, China: Source identification and size distribution. Atm. Environ. 105:53-60.

Tittarelli A, Borgini A, Bertoldi M, De Saeger E, Ruprecht A, Stefanoni R, Tagliabue G, Contiero P, Crosignani P (2008) Estimation of particle mass concentration in ambient air using a particle counter. Atmos. Environ. 42:8543−8548.

United Nation (2018) World Urbanization Prospects 2018. https://population.un.org/wup/. Accessed 08 January 2019.

Wang H, Shi H, Li Y, Yu Y, Zhang J (2013) Seasonal variations in leaf capturing of particulate matter, surface wettability and micromorphology in urban tree species. Front. Environ. Sci. Eng. 7(4): 579–588

Wang L, Gong H, Liao W, Wang Z (2015) Accumulation of particles on the surface of leaves during leaf expansion. Sci. Total Environ. 532:420–434.

Weerakkody U, Dover JW, Mitchell P, Reiling K (2018) Quantification of the traffic-generated particulate matter capture by plant species in a living wall and evaluation of the important leaf characteristics. Sci. Total Environ. 635:1012–1024.

Wilkinson KE, Lundkvist J, Netrval J, Eriksson M, Seisenbaeva GA, Kessler VG (2013) Space and time resolved monitoring of airborne particulate matter in proximity of a traffic roundabout in Sweden. Environ. Pollut. 182:364−370.

World Health Organization (2016) Ambient air pollution: A global assessment of exposure and burden of disease. http://www.who.int/iris/bitstream/10665/250141/1/9789241511353-eng.pdf. Retrieved 20 November 2016.

Yan J, Lin L, Zhou W, Han L, Ma K (2016) Quantifying the characteristics of particulate matters captured by urban plants using an automatic approach. J. Environ, Sci. 39:259 –267.

Yin J, Allen AJ, Harrison RM, Jennings RG, Wright E, Fitzpatrick M, Healy T, Barry E, Ceburnis D, McCuske D (2005) Major component composition of urban PM10 and PM2.5 in Ireland. Atmospheric Res. 78:149–165.